

# Single-Photon Interference

Liza Mulder\* and Isabel Lipartito<sup>†</sup>

*Department of Physics, Smith College, Northampton, MA 01063*

(Dated: December 12, 2014)

## Abstract

It has been understood since the 19th century that light displays both wavelike and particle-like properties. Light beams of differing phase interfere with each other and create observable light and dark fringes, as seen in Young's Double Slit experiment. At the same time, light can be seen as a particle: quanta of light, or photons, excite electrons to higher states of energy as seen in the photoelectric effect. It is unlawful to attempt to classify light as a single entity. We demonstrate the dual nature of light in the Single Photon Interference Experiment- a variation of Young's Double Slit Experiment. We use a beam of light and a double slit apparatus with the confirmation that, within a certain probability, there is only a single photon in flight through the double slit device at any time. Considering light to be a particle, we would expect to see two single bright fringes projected onto a screen. However, even in the case of a single photon in flight at once, we still see dark and light interference fringes. In this paper, we discuss the revolutionary implications of this result as well as how we might model these interference patterns. We fit the Fresnel and Fraunhofer models of interference to our data and discuss the advantages and disadvantages of each. We find that each fit models certain aspects of our data better than the other. The Fresnel model better predicts overall shape and behavior near the bottom and the edges of the plots. The Fraunhofer model better predicts the height, width, and spacing of the peaks. Together they fit our data very well, given our estimates of the experimental parameters. Our ten parameters and the values we gave them are listed in Table I. The resulting reduced chi-square values for our fits are in Table II. The Fraunhofer reduced chi-squared values were: double-slit 57.67, far slit 3.31, near slit 0.326. The Fresnel reduced chi-squared values were: double-slit 5.99, far slit 3.45, near slit 4.45. None of our fits were ideal, but except for the Fraunhofer double-slit the reduced chi-square values remained under 6. From this we conclude that we could be more precise in applying our fits by integrating over those parameters which were not strictly constant but had a range. The Fresnel model, at least, we discovered is very sensitive to these small changes.

## I. INTRODUCTION

Isaac Newton believed defining light as a particle-like quantity (calling them corpuscles) would explain light refraction and reflection<sup>1</sup>. Interference experiments by Young in the early 19th century opposed the ideas of Newton and demonstrated the apparent wavelike nature of light. Young sent a single coherent beam of light through a double slit apparatus and observed a resultant interference pattern. In the latter part of the 19th century, discoveries by Maxwell, Faraday, and Hertz lead to the unification of the theories of electricity and magnetism. Light was realized to be an electromagnetic wave. The contemporary theories of light bore little resemblance to the corpuscular theory of Newton.<sup>2</sup>

Further discoveries in the early 20th century, however, demonstrated the particle nature of light. Perhaps the most famous example of this is Einstein's Nobel Prize-winning explanation of the photoelectric effect. Einstein explained that quanta of light, called photons, strike the surface of a metal plate and excite electrons to freedom<sup>5</sup>. The advent of quantum mechanics, a field based largely off the quantized nature of electromagnetic energy, further explored the particle-like properties of light. A further example of this is Compton Scattering- a effect where a photon elastically collides with an electron and experiences a shift in wavelength.

We know now that light exhibits particle-like properties: photons scatter and collide with matter. We also know light exhibits wave-like properties: light beams constructively and destructively interfere with each other. But can we say that we understand light? The best way to test our understanding is to undertake the Single Photon Interference Experiment. We will take the same general set up as for the Young Double Slit Experiment: beam of light, double slit, and means of viewing the output (see Methods section for a detailed description). However, this time, we will reduce the intensity of light that we can be sure, to within a certain probability, that there is only a single photon in flight through the double slit apparatus at any time.<sup>4</sup>

In this paper, we perform the Single Photon Experiment and examine the output double slit interference pattern produced by single photon interference. We fit our output to two different models: the Fraunhofer model and the Fresnel model, which draw upon different approaches to model the behavior of light. The Fraunhofer model makes use of the picture of light as a plane wave reaching the two slits and propagating through it as a wave. The Fresnel model considers the phase variation of an electromagnetic field with position in that

field. The Fresnel model is a sum of the amplitudes over multiple paths from one location to another (here, from the source to the detector). We discuss these models and our found fits in our analysis section.

## II. METHODS

### A. Apparatus

We used the Teach-Spin “2-Slit Interference One Photon at a Time” Apparatus for this experiment.

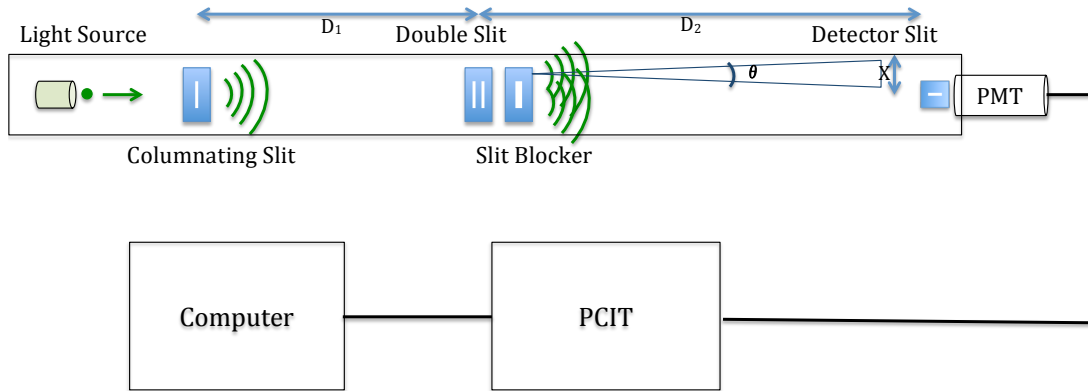


FIG. 1. Teach-Spin apparatus to measure quantum interference: a 1m-long black box containing an adjustable light source (about 550nm), columnating single slit, double slit, slit blocker, detector slit, and photomultiplier tube (PMT) detector. We sent the PMT output to a pulse-counter interval timer (PCIT), and from there to the computer.

The apparatus comes with a long black box containing an adjustable light source (with green filter to restrict wavelength and intensity), a 670nm laser source for alignment, four magnetic slit-holders along the length of the box for adding slits in the path of the light, and two detector options at the end: a photodiode (for laser light) and a photomultiplier tube (for lightbulb illumination). The set-up is shown in Figure 1. We placed a single columnating slit in the first holder to focus the light from the lightbulb. This created vertical a single-slit diffraction pattern, which we centered on the next set of slits. In the second slit holder, in the middle of the box, we placed the double-slit, and immediately following that we placed

the slit blocker (a wide single-slit) so we could choose to allow light through one slit, both slits, or neither. At the far end of the box we placed a single slit for the detector slit - by moving this slit holder lengthwise across the channel we could "scan" the interference pattern and measure photon counts at regular intervals.

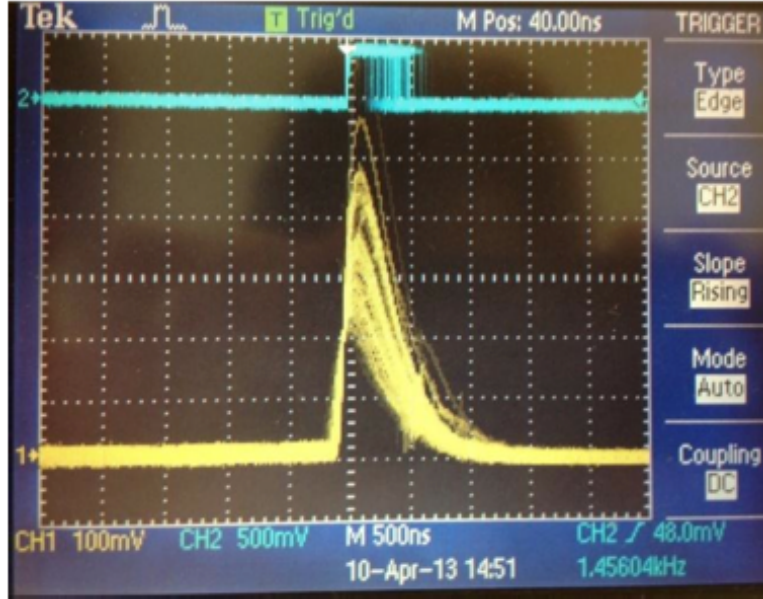


FIG. 2. The Pulse Counter Interval Timer (PCIT) works by comparing input pulses to a threshold voltage, and generating a square wave pulse of 5V for those above the threshold, and 0V for those below. The result is that the irregular peaks of different height and shape from the photomultiplier tube (the yellow traces) are translated into a square wave (the blue trace), and the number of peaks in the square wave are counted for a given time interval.

Behind the detector slit was a photomultiplier tube (PMT). A PMT utilizes the photoelectric effect to detect incoming particles. When photons hit the PMT, they release electrons from the metal. The PMT voltage, applied across the 10 plates of the device, accelerates the freed electrons until they impact the next plate. This continues, with the number of electrons increasing at each step, until a detectable pulse of electrons reaches the end of the PMT. The PMT voltage determines how much initial energy a particle needs to cause the cascade of electrons - slow-moving particles won't reach the next plate with enough energy to release electrons, and changing the PMT voltage changes that cut-off point. The end of the PMT is connected across a resistor to ground - the voltage across this resistor is proportional to the current going through it, and the current depends on the pulse of

electrons generated in the PMT. In this way a PMT generates a voltage in response to the arrival of a photon. Adjusting the PMT settings changed the sensitivity - a low setting missed lower-energy photons, but a higher setting generated more noise. We optimized this setting (got the best signal-to-noise ratio) at 600V.

The short "pulse" from the PMT was output as a voltage spike, which we sent to the pulse counter interval timer (PCIT). The PCIT had a "discriminator" which screened out all pulses below a threshold voltage (in order to remove low energy noise, at the expense of some lower-energy photons) - we optimized this setting at 0.6V. The PCIT kept count of how many voltage "pulses" above its threshold voltage it received from the PMT within a 10s, 1s, or 0.1s time interval. (See Figure 2 for an oscilloscope image of the conversion from voltage spike to square wave.) More photon detections within the time interval indicated a high light intensity at that position of the detector slit, and photon detection levels near the background indicated a dark fringe in the pattern. By optimizing the apparatus alignment and the PMT and PCIT settings, we obtained a signal to noise ratio of roughly 4000 at the brightest point in the pattern.

## B. Optimization

We optimized two settings in our set-up: the PMT voltage, and the PCIT discriminator voltage. We measured photon counts recorded by the PCIT with the shutter open and the shutter closed for various settings. The shutter open was our "signal + noise" measurement, and the shutter closed was just "noise." By taking the ratio we got an estimate for the signal+noise/noise ratio ( $S+N/N$ ) of our data. We first kept PMT voltage constant while varying discriminator setting. The  $S+N/N$  ratio would increase and then decrease, allowing us to find the best discriminator setting for each PMT voltage. We then changed the PMT voltage and found the next peak  $S+N/N$  value. From a previous module we knew the optimal PMT voltage for our apparatus would be between 600V and 900V, and the optimal discriminator setting below 3V. We started our measurements near the optimized settings of the previous group to use the equipment, and so quickly found one setting which stood out as drastically better than the others. All our  $S+N/N$  values stayed below 800, except for one which was around 4000. For a 10s counting interval we'd get around 40,000 counts with the shutter open and about 10 counts with it closed. This occurred at 600V (read off the

PMT dial) and 0.6V for the discriminator setting. It is important to note that the voltage we read from the dial of the PMT did not match the value measured with a DMM, and that none of the set-ups in the lab had the same voltages even if we used the same setting. So this value will have to be found for each apparatus.

### C. Data Collection

Our green light bulb-power setting was at 5, which correlates to approximately  $10^3$  photon events per second. Green light photons have wavelengths near  $0.55\mu$  meters. The time in flight of the photons is on the order of nanoseconds (divide the meter of distance they travel by their speed,  $c$ ). Separation time between successive arrivals is on the order of milliseconds (an average measurement of  $10^3$  photons per 1s time interval gives an average time between arrivals of  $10^{-3}s$ ). The PCIT will be devoid of photons over 99 percent of the time, even given that photon emissions are random events and therefore more likely to occur close together. The ratio of flight time to average photon separation time is  $10^{-9}s \div 10^{-3}s = 10^{-6}$ . Therefore there is a very low probability that more than one photon will be in the apparatus at any given time, for the duration of our experiment.

To collect data, we moved the detector slit in increments of 0.1mm across the width of the interference pattern, measuring the photons counted for a 1s interval at each position. We called the position of the detector slit  $X$ , and it relates to the angle from the central maximum of the pattern ( $\theta$ ) by the formula  $\theta = \frac{X-X_0}{D_2}$ , where  $X_0 = 3.95mm$ ,  $D_2 = 500mm$ , and we have applied the small angle approximation  $\sin(\theta) = \theta$ . Figure 1 shows these variables and what they refer to in the set-up, and Table I gives all parameter values.

The apparatus came with a micrometer which moved the detection slit holder 0.5mm every turn, and allowed us to read the slit's current position from the barrel. In this way we could measure the photon counts at different positions. We repeated this process with the slit blocker in different positions: once blocking the near slit and scanning the single-slit diffraction pattern generated by the far slit, once blocking the far slit and scanning the pattern produced by the near slit, once with both slits unblocked, and once with both slits blocked to get a read of the background. We did three runs for each position of the slit blocker, to get a measure of the scatter in the results.

Due to the random nature of the phenomena, and the method of data collection, we

could not obtain an uncertainty for individual measurements we instead calculated error from the data for the three runs with the same settings. That is, for each position of the blocking slit, we took data spanning the interference pattern three times. This gave us three sets of data to compare which should have been the same except for random scatter. We tried calculating uncertainty using the relationship between uncertainty and average value in Poisson statistics (which governs random events), but we were not sure if our count rate had become too high and we had ventured into the realm of Gaussian statistics. To test this, we calculated the average value, standard deviation, and square root of the average value for every position of detector slit within each set of three runs. We compared the standard deviation with the square root of the average in excel, and found that they differed by sometimes a factor of 10. We decided to use the standard deviation as our error for the rest of the analysis.

We then analyzed this data and compared it to two theoretical models with Mathematica.

### III. RESULTS

The main result of our experiment was that we did indeed see single slit and double slit interference patterns, as we expected. We then we fit two models to the data, to quantitatively verify our observation and agreement with theory. Figures 3 and 4 show the detected light intensity (measured by the number of photon counts per second) at sequential micrometer settings (which give the position of the detector slit). The red data points are our raw data, showing the scatter across three runs, as well as the general trend. The larger, blue data points are the average values with error bars (the mean and standard deviation of the values from the three runs) for each value of position. Our data has the form of single and double slit diffraction patterns, qualitatively. In the analysis section we compare our data to two theoretical models.

### IV. ANALYSIS

Below, we discuss the two models and our fits, as well as the goodness of these fits and their implications for this experiment and the theory of light.

We calculated fits for both the Fraunhofer Model and the Fresnel Model. The two are

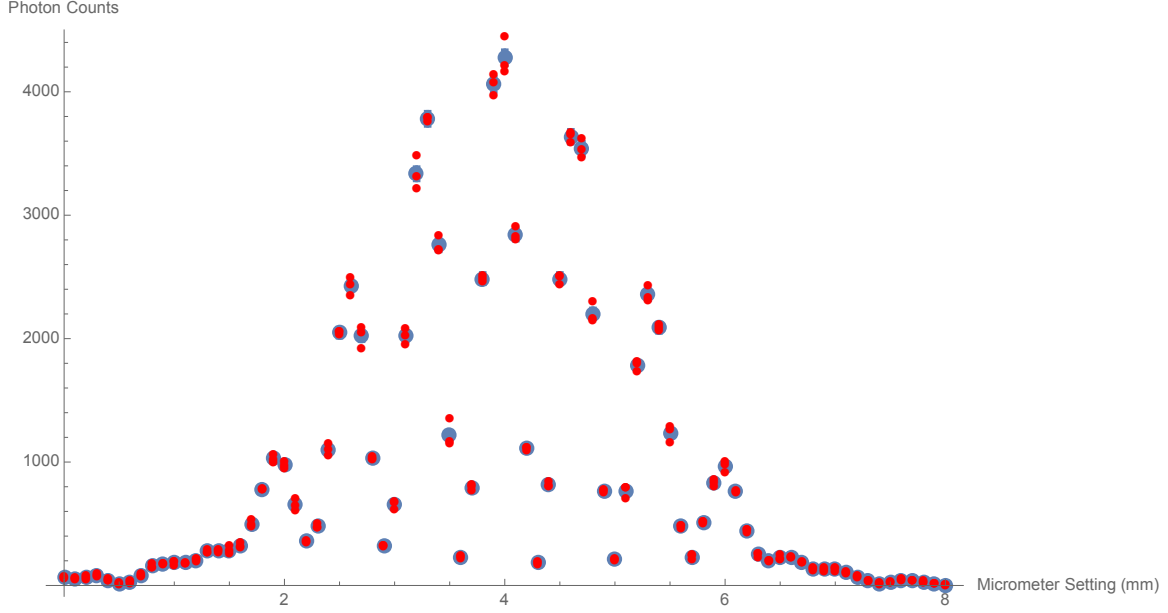


FIG. 3. Our data for the double slit pattern. Raw data is the small red points, averages with standard error are the larger blue points with error bars.

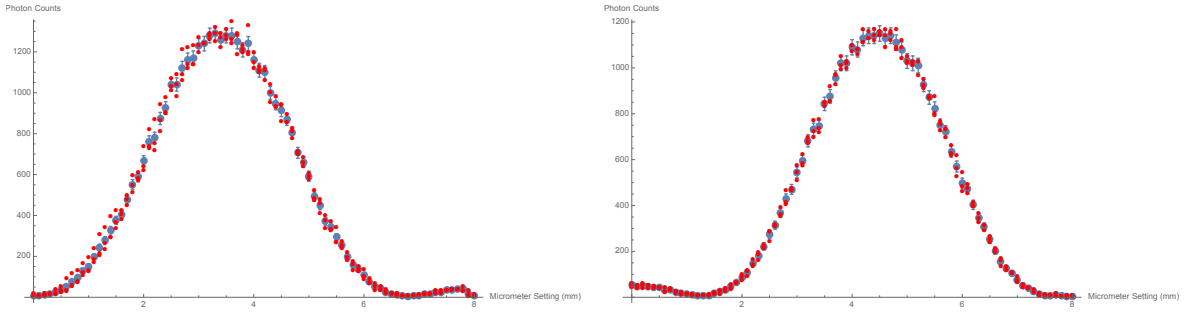


FIG. 4. Our data for the single slit patterns. Raw data is the small red points, averages with standard error are the larger blue points with error bars.

approximately applied in different regimes, determined by the Fresnel number:  $F = \frac{a^2}{\lambda L}$ .  $\lambda$  is the wavelength of the incident photons,  $a$  is the slit width, and  $l$  is the distance from diffracting slits to the detector slit. When  $F \ll 1$  the small slit is far from the detector screen, and the Fraunhofer model can be used as an approximation of the Fresnel model. Nearer to the slit, where  $F \approx 1$ , the Fresnel model is more relevant to the behavior of the light. <sup>3</sup> The Fresnel number for our experiment is roughly  $\frac{(0.1mm)^2}{555nm*500mm} \approx .036$ . Therefore the Fraunhofer model should be more appropriate, though neither is quite right - we would have to use a longer box, a longer wavelength light source, or thinner slits, to make the



Fresnel number much smaller than 1.

### A. The Fraunhofer Model

The Fraunhofer Model treats light as a wave and models it's arrival at a plane very far away. This is called "far field." It uses the assumption that the distance between the plane of the slit and the detector plane is much greater than the features of the slits or of the diffraction pattern. This assumption allows the integral of complex exponentials which exactly describes the situation (shown later in the Fresnel model) to be approximated by the following sinusoidal equations, which are simpler.<sup>3</sup>

For the double slit case, the equation simplifies to:

$$I_{double} = I_0 \left( \frac{\sin(\frac{\pi a}{\lambda} \sin(\frac{x-x_0}{D_2}))}{\frac{\pi a}{\lambda} \sin(\frac{x-x_0}{D_2})} \right)^2 \times \cos\left(\frac{\pi d}{\lambda} \sin(\frac{x-x_0}{D_2})\right)^2 \quad (1)$$

For the single slit cases, the equations are:

$$I_{far} = \frac{I_0}{4} \left( \frac{\sin(\frac{\pi a}{\lambda} \sin(\frac{x-x_1}{D_2}))}{\frac{\pi a}{\lambda} \sin(\frac{x-x_1}{D_2})} \right)^2 \quad (2)$$

$$I_{near} = \frac{I_0}{4} \left( \frac{\sin(\frac{\pi a}{\lambda} \sin(\frac{x-x_2}{D_2}))}{\frac{\pi a}{\lambda} \sin(\frac{x-x_2}{D_2})} \right)^2 \quad (3)$$

Where  $I_0$  is the intensity of the central maximum,  $a$  is the width of the slits,  $x_0$  is the location of the central maximum in the double-slit pattern,  $x_1$  is the location of the central max in the far single-slit pattern,  $x_2$  is the location of the central max in the near single-slit pattern,  $D_2$  is the distance between the slit and the detector,  $\lambda$  is the wavelength of the light,  $x$  is the position of the detector slit,  $c$  is a vertical offset, and  $d$  is the slit separation from slit center to slit center.

We fit our data to the Fraunhofer model by plotting our entire data set against the model, using the manufacturer's values for the slit widths, slit separation, and light wavelength, and our observed maximum intensity and central maximum locations. We then modified these values to try and get a better fit of the function to the data, estimating a satisfactory fit by eye. As the manufacturer did not give error for most of their parameters, we had to guess at the limits within which we could vary the parameter values (see Table I). However, we obtained a good fit for the double slit pattern (with the exception of the very edges), and

decent fits for the single slit patterns. Our single slit data was slightly off because we had not centered the columnated light exactly on the two slits, so one slit had approximately 10% more illumination than the other. As the fit assumed equal illumination from both slits, the amplitudes did not match.

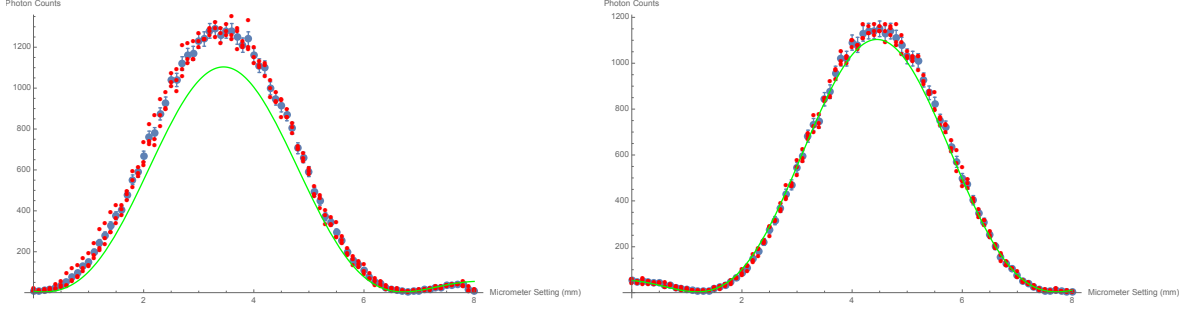


FIG. 5. Our data for the single slit patterns with the Fraunhofer formula on top. The parameters we used are in Table I. Raw data is the small red points, averages with standard error are the larger blue points with error bars.

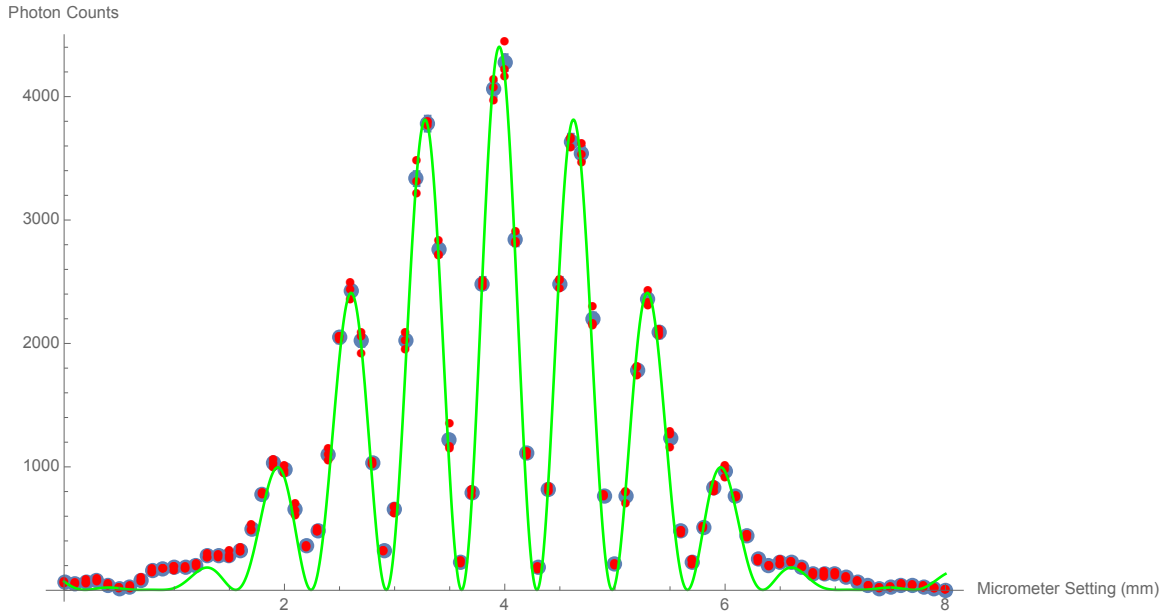


FIG. 6. Our data for the double slit pattern with Fraunhofer fit on top. Raw data is the small red points, averages with standard error are the larger blue points with error bars.

TABLE I. Parameter values for our fits. We started with the values given in the apparatus manual ( $a, d, \lambda$ ), measured ( $D_1, D_2$ ), or estimated from the plots ( $I_0, x_0, x_1, x_2, c$ ). We then optimized (within the uncertainty for each parameter) to get the Fraunhofer fits as close to the data as possible.

Parameter	Fit value	Original values
Counts/sec at central max $I_0$	4400 counts/sec	4000 counts/sec
Slit width $a$	0.085 mm	0.1 mm
Slit separation $d$	0.406 mm	0.406 mm
Light wavelength $\lambda$	555 nm	541 nm - 551 nm
Location of central max (double slit) $x_0$	3.95 mm	4.0 mm
Location of central max (far slit) $x_1$	3.45 mm	4.0 mm
Location of central max (near slit) $x_2$	4.45 mm	4.0 mm
Offset $c$	3.6 counts/sec.	0 counts/sec
Distance from columnating slit to diffracting slits $D_1$	338 mm	380 mm
Distance from diffracting slits to detector slit $D_2$	500 mm	500 mm

## B. The Fresnel Model

The Fresnel model does not use the approximation from the Fraunhofer model, as the Fresnel model does not assume that we are in the “far field” limit. The Fresnel model works in the near-field regime, where the Fraunhofer model does not. The Fresnel model is a more accurate model for all regimes. Therefore the equation is left in it’s complex exponential form, and the distances between the slits and between slit and detector become very important. <sup>3</sup> This equation is very difficult to solve, but a computing program such as Mathematica can run the calculation.

The factor of 42.044 is a proportionality constant we calculated to fit the Fresnel model to our data. It is the ratio of the maximum resultant intensity from the Fresnel model to the maximum intensity value of our experiment. The Fresnel model sum over paths approach gives us amplitudes (resulting from the integral), and we need to take their absolute square to find the intensities. The limits in the integral sum over the width of each slit in the double-slit, assuming that the distance between slits  $d$  is measured from centers.

The single slit cases:

$$I_{near} = I_0 * 42.044 * |e^{\frac{2\pi i D_1}{\lambda}} * e^{\frac{2\pi i D_2}{\lambda}} * \int_{x_0 + \frac{d}{2} - \frac{a}{2}}^{x_0 + \frac{d}{2} + \frac{a}{2}} e^{\frac{2\pi i (x_0 - y)^2}{D_1 \lambda}} * e^{\frac{2\pi i (y - z)^2}{D_2 \lambda}} dy|^2 \quad (4)$$

$$I_{far} = I_0 * 42.044 * |e^{\frac{2\pi i D_1}{\lambda}} * e^{\frac{2\pi i D_2}{\lambda}} * \int_{x_0 - \frac{d}{2} - \frac{a}{2}}^{x_0 - \frac{d}{2} + \frac{a}{2}} e^{\frac{2\pi i (x_0 - y)^2}{D_1 \lambda}} * e^{\frac{2\pi i (y - z)^2}{D_2 \lambda}} dy|^2 \quad (5)$$

The double slit case is simply the sum of the waveforms generated by each slit (after their absolute square has been taken to convert amplitudes into intensities):

$$I_{double} = I_{near} + I_{far} \quad (6)$$

The parameters have the same meanings as in the Fraunhofer model, with the addition of  $D_1$ , the distance from the columnating slit to the diffracting slit, and with the exception of  $x$ ,  $y$ , and  $z$ :  $x$  is the location of the columnating slit,  $y$  is the location of the diffracting slit, and  $z$  is the location of the detector slit. Figure 7 shows the parameters and their use in the Fresnel model.

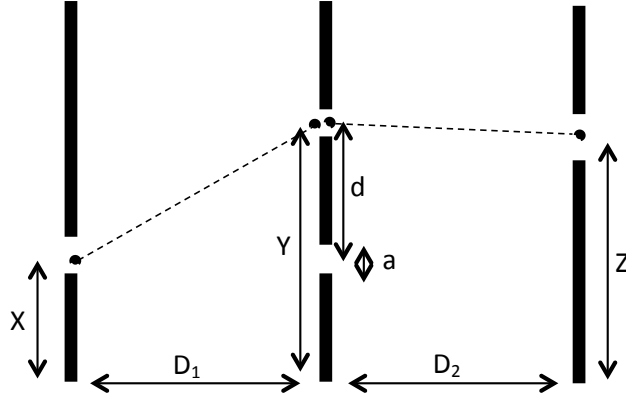


FIG. 7. The set-up and variables used in the Fresnel Approximation. Note that the variable "Z" in the Fresnel formula is what we've been calling "X" in our other calculations - the position of the detector slit.

After fitting our data, we computed the reduced chi-square value for each fit (see Table II). All few of the values were very large. By examining the distance of individual points from the fit, however, we realized that the majority actually had small deviations from the line, with a few outliers which weighted the fit. Even so, from the graphs it is clear that

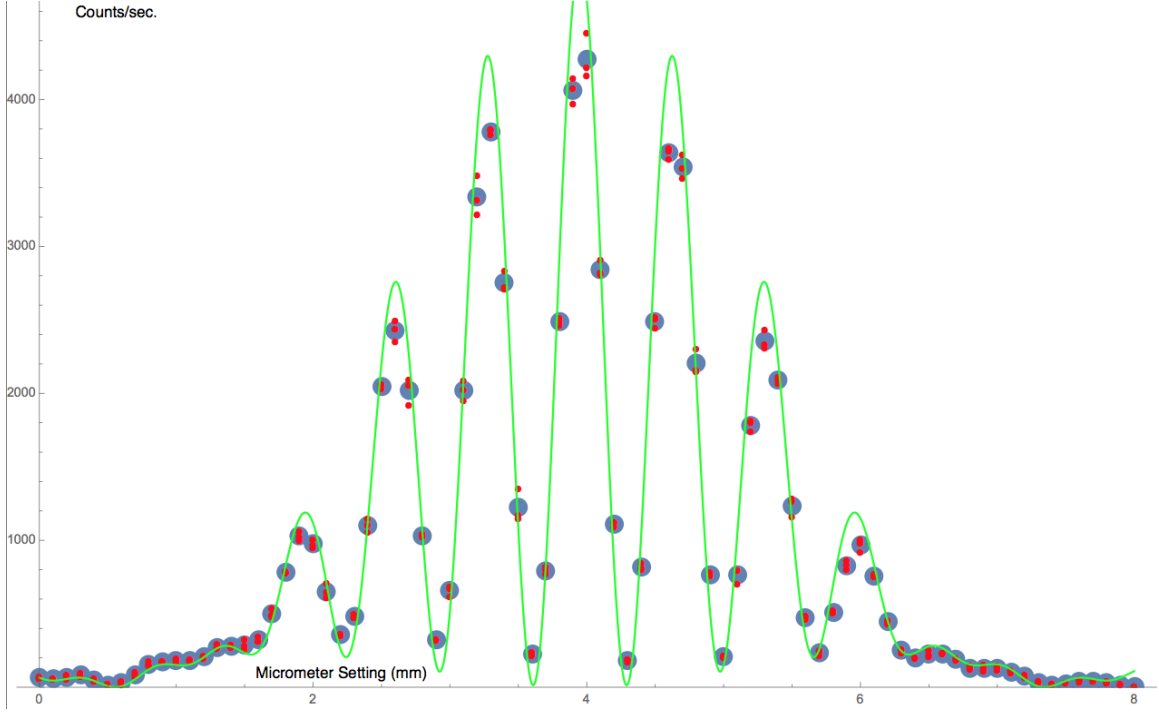


FIG. 8. Our data for the double slit pattern with Fresnel fit on top. Raw data is the small red points, averages with standard error are the larger blue points with error bars.

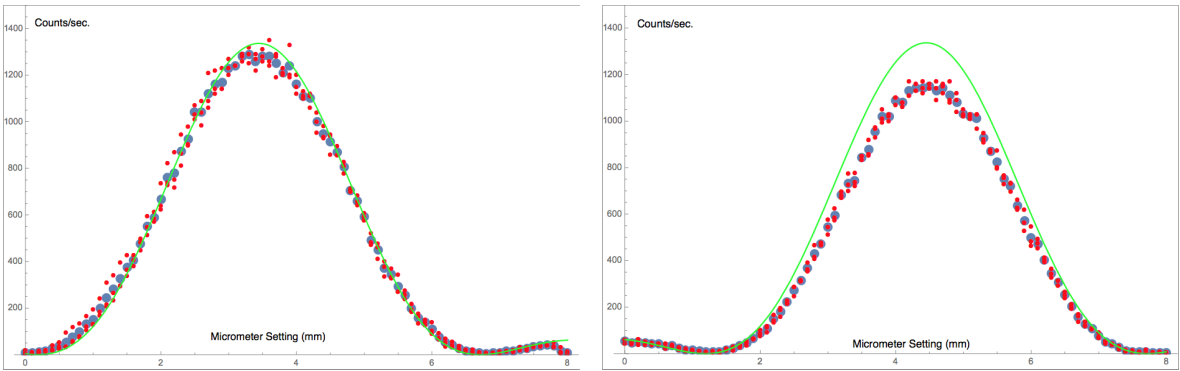


FIG. 9. Our data for the single slit patterns with the Fresnel formula on top. The parameters we used are in Table I. Raw data is the small red points, averages with standard error are the larger blue points with error bars.

no single set of parameter values allows all the fits to match the data. We optimized our parameters for the Fraunhofer double-slit fit - as these parameter values were within the uncertainty of what we knew they should be, we kept these parameters. However, the other fits each had some sort of systematic offset from the line.

TABLE II. Reduced chi-square values for our fits.

Fraunhofer	Double Slit	57.67
	Far Slit	3.31
	Near Slit	0.326
Fresnel	Double Slit	5.99
	Far Slit	3.45
	Near Slit	4.45

## V. DISCUSSION

Our biggest question with this experiment was why, while we obtained clear data of the interference patterns, these results deviated from the theoretical models. In particular the Fraunhofer model could not be made to fit our data very well at the edges, and the Fresnel got the general shape but the widths and heights of the peaks didn't quite match, even with the best estimations of our parameters.

In addition, we observed that the Fresnel model fit very well at the very edges of our pattern: it was able to follow the subtle bumps and wiggles of that region. The Fresnel model also replicated the "wavy offset" of our minima, while the Fraunhofer model had each minima come down to zero. This offset was several times too large to be attributed to our background noise, so it is likely due to some characteristics of the Fresnel model which the Fraunhofer model approximated away. The Fraunhofer model did better in the middle- around the more defined light and dark fringes. The Fresnel model does not fit the inner light and dark fringes very well. Most of the peaks are too tall and a bit too wide in consequence. We are not exactly sure why this is so, but we have a few speculations. The Fraunhofer model is designed to take advantage of the wave nature of light, and is not equipped to handle any 'edge effects' resulting due to the finite nature of the detector slit. The Fresnel model, on the other hand, is a sum of the amplitudes over all paths from the source to the detector, and is more equipped to take into account imperfect paths and imperfections around the edges of the pattern. So the Fresnel model gave a more accurate picture of the general shape of the graph, while the Fraunhofer model better predicted the height and spacing of the peaks, as it was designed to do.<sup>4</sup>

In order to better gauge the fits of the models to the experimental data, we would want to repeat this experiment using smaller incremental turns of the micrometer. There are large gaps in our plotted fits that could be closed with tighter measurements. We possibly would want to turn the micrometer by .05 mm instead of .1 mm increments. We would also want to more precisely measure ourselves the parameters that went into our Fraunhofer and Fresnel fits: slit width ( $a$ ), slit separation ( $d$ ), and the distances from the different slits to the detector slit ( $D_1$  and  $D_2$ ), rather than relying on the uncertain reported values from the Two-Slit Interference, One Photon at a Time manual. We could also gauge some error estimates for these values and propagate them, in our fits, so our fits would themselves have an error range. We could try to get a better idea of the range of wavelengths produced by the filtered light-bulb, and maybe integrate over those values. We could also integrate over the width of the columnating source slit. However, the computation time might be too prohibitive.

An interesting project would be to continue this experiment and made adjustments to bring the set-up closer to the Fraunhofer and Fresnel limits. For Fraunhofer, we would want to repeat this experiment with thinner slit widths, larger wavelength photons, and a longer box. For Fresnel, we would want to repeat this experiment with larger slits, shorter wavelength photons, and a shorter box. Taking into account practicality, we could adjust the Fresnel number in both cases to ensure we are in the correct regime for our data to resemble the Fraunhofer or Fresnel model. It would be exciting to confirm the Fraunhofer and/or Fresnel model, and probe the limits of these models further.

Regarding the quantum mechanical theory of this experiment, we did indeed observe single photon interference. If a single photon was moving through a two-slit apparatus at any one time, how did the interference happen? It seems like the photon somehow 'knew' about the two slits and managed to self-interfere (a bit of an obfuscating idea!). It is certainly unfair to continue to think of the photon as a classical particle or classical wave propagating through space. Perhaps it is better to think of a sort of quantum amplitude propagating through space- an amplitude whose absolute square would give information on where and when one is likely to observe the photon interaction event. The picture by which we observe the photon events are the double slit interference patterns which depict favored and not-so-favored photon detection spots (according to the propagating quantum amplitude) as light and dark interference fringes, respectfully.<sup>4</sup>

The double slit experiment may be rather old, but it is certainly still relevant today. Contemporary physicists are exploring the wave-particle duality of other particles aside from photons. In 1999, the double slit experiment was successfully performed with buckyballs and it has been relatively recently been performed with electrons.<sup>6</sup> The application of quantum mechanics to explain the behavior of subatomic particles and their interactions via fields, known as quantum field theory (QFT), is a new and relevant division of physics. Contemporary research in Quantum Electrodynamics, the QFT to explain the interaction of light and matter, involves introducing a wave function for the photon and mathematically modeling interactions between matter and light<sup>7</sup>. Quantum field theory might help us probe the nature of the photon and better understand its seemingly 'impossible' doings.

## VI. CONCLUSION

We successfully performed the single photon interference experiment and observed the expected single-slit diffraction patterns and double-slit interference patterns predicted by theory. We fit our resulting data to the Fresnel and Fraunhofer models and found that the both models fit different aspects of the data. The reduced chi-square values for the Fresnel model were more consistent than those for the Fraunhofer model, and this reflects the goodness of fit seen in the plots. The Fresnel model overall better predicts the shape of the data, and is more sensitive to the details of the apparatus. The Fraunhofer predicts what it was designed to predict - the light and dark fringe height, width, and spacing, treating light as a wave and the set-up as ideal. We explored the quantum mechanical implications of single photon interference and discussed quantum electrodynamics, a theory developed to apply quantum mechanics to the electromagnetic field and better physically and mathematically understand the mysterious nature of the photon.

---

\* emulder@smith.edu

† iliparti@smith.edu

<sup>1</sup> Use of Hamilton's Canonical Equations to Rectify Newton's Corpuscular Theory of Light: A Missed Opportunity. Buenker et al, 2004. Sov. J. Chem. Phys. 22 (2003) 124

<sup>2</sup> Introduction to Electrodynamics, 4th Edition. David J. Griffiths, 2012. Addison Wesley.



- <sup>3</sup> Weisstein, Eric W. Wolfram Science World, "Fraunhofer Diffraction," "Fresnel Diffraction," "Fresnel Number." 2007.
- <sup>4</sup> TeachSpin Instruction Manuals. Two-Slit Interference, One Photon at a Time (TWS1-B). TWS1B-PCIT1 Instruction Manual. Rev. 1.0 6/2013
- <sup>5</sup> Six Ideas That Shaped Physics: Unit Q - Particles Behaves Like Waves. Thomas Moore. McGraw-Hill Science/Engineering/Math; 2 edition, 2003.
- <sup>6</sup> Wave-Particle Duality of C60 Molecules. Arndt et al, 1999. Nature Vol. 401
- <sup>7</sup> The Photon Wave Function. Iwo Bialynicki-Birula, 1996. Coherence and Quantum Optics VII, Eds. J. H. Eberly, L. Mandel, and E. Wolf Plenum, New York 1996, p. 313

## VII. APPENDIX

Below is the Mathematica code we used to calculate the Fresnel and Fraunhofer fits, and the Chi Square values.

We first used the "Import" function to import our raw data as csv files. It is important that each file only contain a list of x,y pairs or you will get an error when you try to make a plot. We used the compiled raw data from the three runs for the double slit, far slit, and near slit runs, as well as a list of average values and a list of standard deviations for each one. With these datasets we used "ListPlot" and "ErrorListPlot" to make plots of the raw data superimposed on the averages with error bars. (See Figures 3, and 4).

We then defined all the parameters which would be needed in the fits:  $I_0, a, d, \lambda, x_0, x_1, x_2, c, D_1, D_2$ .

We defined our fit formulas as follows:

Fraunhofer double-slit:

```
g[x_] := I0*0.25*((Sin[
Pi*a*Sin[(x - x0)/D2]/(lambda)]*(lambda/(Pi*a*Sin[(x - x0)/D2]))^2)*(Cos[
Pi*d*Sin[(x - x0)/D2]/lambda]^2) + c;
```

Fraunhofer far-slit:

```
h[x_] := I0*0.25*((Sin[
Pi*a*Sin[(x - x1)/D2]/(lambda)]*(lambda/(Pi*a*Sin[(x - x1)/D2]))^2) + c;
```

Fraunhofer near-slit:

```
k[x_] := I0*0.25*((Sin[
Pi*a*Sin[(x - x2)/D2]/(lambda)]*(lambda/(Pi*a*Sin[(x - x2)/D2]))^2) + c;
```

Fresnel near-slit:

```
slit1[z_] :=
E^((2*\[Pi]*I*D1)/lambda)*E^((2*\[Pi]*I*D2)/lambda)*
Integrate[
E^((\[Pi]*I*(x0 - y)^2)/(D1*lambda))*E^((\[Pi]*I*(y - z)^2)/(
D2*lambda)), {y, x0 + (d/2) - (a/2), x0 + (d/2) + (a/2)}]
```

```
s1[z_] := 42.044*I0*Re[slit1[z]*Conjugate[slit1[z]]]
```

Fresnel far-slit:

```
slit2[z_] :=
E^((2*\[Pi]*I*D1)/lambda)*E^((2*\[Pi]*I*D2)/lambda)*
Integrate[
E^((\[Pi]*I*(x0 - y)^2)/(D1*lambda))*E^((\[Pi]*I*(y - z)^2)/(
D2*lambda)), {y, x0 - (d/2) - (a/2), x0 - (d/2) + (a/2)}]
```

```
s2[z_] := 42.044*I0*Re[slit2[z]*Conjugate[slit2[z]]]
```

Fresnel double-slit:

```
slit[z_] :=
42.044*I0*Re[(slit1[z] + slit2[z])*Conjugate[(slit1[z] + slit2[z])]]
```

To plot our fits, raw data, and average values with error bars, we used the “Plot” function (for the fits), “ListPlot” function (for the raw data), and the “ErrorListPlot” function (for the averages with error bars) to make the plots, and the “Show” function to plot them on the same graph. For example:

```
Needs["ErrorBarPlots"];
data2Slit = Import["...4.45mmAll.csv"];
data2SlitAvg = Import["...4.45mmAvg.csv"];
```

```

data2SlitError = Import["...4.45mmError.csv"];
dataPlot2SlitAvg = ErrorListPlot[Table[
{data2SlitAvg[[i]],data2SlitError[[i]]},{i,1,81}], PlotRange -> {0, 4800}];
dataPlot2Slit = ListPlot[data2Slit, PlotMarkers -> {Automatic, 8}, PlotStyle -> Red];
fita = Plot[slit[z], {z, 0, 8}, PlotStyle -> Green];
Show[dataPlot2SlitAvg, dataPlot2Slit, fita]

```

To do the Reduced Chi Squared calculations, we needed the raw data with just the y-values. We made new .csv files and imported them. It was important to use the “Flatten” function enclosing the “Import” function to get rid of the outer brackets Mathematica automatically puts around lists and tables.

We also needed a list of values from the fit to compare to our data. We used the “Table” function enclosed again in “Flatten” to get a list of values from the functions above.

```

dataNearFraun = Flatten[Table[k[x],{x,0,8,0.1}]];
dataFarFraun = Flatten[Table[h[x],{x,0,8,0.1}]];
dataDoubleFraun = Flatten[Table[g[x],{x,0,8,0.1}]];
dataNearFres = Flatten[Table[s1[z], {z, 0, 8, .1}]];
dataFarFres = Flatten[Table[s2[z], {z, 0, 8, .1}]];
dataDoubleFres = Flatten[Table[slit[z], {z, 0, 8, .1}]];

```

Our reduced chi square function is below:

```

redchisq[data_, dist_] :=
Abs[Total[((data - dist)^2)/dist]/Mean[data]]

```

To get the reduced chi squared for a fit, just enter the name of the imported data file as the first argument, and the list of values generated from the corresponding fit as the second argument. Make sure they have the same number of values using the “Length” function, or you’ll get an error.